



Title: Basin-scale connections between reach-scale sediment respiration and point-scale organic-matter decomposition

James C. Stegen^{1,2*}, Morgan Barnes¹, Dillman Delgado¹, Brieanne Forbes¹, Vanessa A. Garayburu-Caruso¹, Amy E. Goldman¹, Maggi Laan^{1,3}, Sophia McKeever¹, Peter Regier¹, Lupita Renteria¹, Scott D. Tiegs⁴

*Correspondence: James.Stegen@pnnl.gov

1. Pacific Northwest National Laboratory, Richland, WA, United States

2. Washington State University, Pullman, WA, United States

3. University of California, Riverside, CA, United States

4. Oakland University, Rochester, MI, United States

Abstract

Stream and river ecosystems play a central role in the movement and decomposition of particulate organic matter, serving as a conduit between terrestrial hillslopes and coastal environments. Microbial-catalyzed decomposition generates simpler organic molecules that fuel respiration, often in the sediments of these ecosystems. However, the degree of connection between sediment-associated respiration (ER_{sed}) and organic-matter decomposition remains poorly understood. How that relationship compares to decomposition's relationship with whole ecosystem (ER_{tot}) and water column (ER_{wc}) respiration is also not clear. We examined the link between particulate organic matter decomposition—using cellulose-based cotton strips as a standardized substrate—and all three components of respiration across 48 sites in the environmentally diverse Yakima River Basin (Washington State, USA). We hypothesized that decomposition within sediments would be most strongly related to ER_{sed} , but decomposition rates were more closely associated with ER_{tot} , with little connection to ER_{sed} or ER_{wc} . This suggests that particulate organic matter decomposition within stream/river sediments reflects integrated system respiration rather than processes confined to sediments or the water column alone. Further, across the basin, decomposition rates nearly spanned the previously reported global range for streams and rivers and were best explained by total dissolved nitrogen (TDN), sediment grain size, and aridity of the upstream drainage area. These results highlight the strong influence of land cover and basin-scale biophysical variation on sediment-associated decomposition processes and indicate that mechanistic models of organic matter decomposition in streams/rivers should account for coupled sediment–water–land interactions.

Introduction

Stream networks are major components of the global carbon cycle (Cole et al., 2007; Drake et al., 2018; Talluto et al., 2024). Whole-stream metabolism is often studied as an integrated outcome of processes occurring across the continuum from the air-water interface down through sediments that are below



the stream itself (Battin et al., 2023; Tank et al., 2010). The sediments include the interface between the streambed and water column (i.e., the benthic zone) and the spatial domain below this interface, referred to as the hyporheic zone (Boulton et al., 1998; Krause et al., 2011; Wondzell, 2011). The benthic zone can be highly productive with significant primary producer (e.g., algae) and heterotrophic microbial biomass (Allan et al., 2021). The hyporheic zone is also highly biogeochemically active due, in part, to surface water flowing through it and mixing with groundwater to stimulate heterotrophic microbial activity (Boano et al., 2014; Lewandowski et al., 2019; Zarnetske et al., 2011). Processes occurring on and around sediments across the benthic-to-hyporheic continuum are often jointly responsible for the bulk of biogeochemical activity in stream systems (Burrows et al., 2017; Fellows et al., 2001; Garayburu-Caruso et al., 2025; Naegeli and Uehlinger, 1997), with important exceptions in large rivers (Roley et al., 2023).

Metabolic processes within integrated stream systems are linked to the building of and breaking down of organic matter (Hall and Hotchkiss, 2017; Odum, 1956). Streams are commonly net heterotrophic whereby they release more carbon than they accumulate (Battin et al., 2023; Bernhardt et al., 2022). This emphasizes the importance of understanding organic-matter decomposition in streams and its connection to respiration rates, which are ultimately linked to rates of elemental cycling. Organic-matter decomposition is commonly measured in stream systems by quantifying the breakdown of specific substrates (Benfield et al., 2017; Woodward et al., 2012). Cellulose-based cotton strips are an increasingly common model substrate for such studies as they enable broad comparisons across streams (and other types of ecosystems) (Colas et al., 2019; Filbee-Dexter et al., 2022; Tiegs et al., 2024; Vyšná et al., 2014). A standard approach is to place them in the field for a known amount of time, retrieve them, and measure the loss in tensile strength, as a proxy for the degree of decomposition. This approach has revealed many factors that impact decomposition in streams such as temperature, land use, aqueous chemistry, sediment texture, stream flow, location within the stream network, and canopy cover, among others (Griffiths and Tiegs, 2016; Tiegs et al., 2024).

Previous studies have examined the relationship between organic matter decomposition and whole-stream respiration (Mancuso et al., 2023; Pingram et al., 2020; Young and Collier, 2009), but have not specifically tied organic matter decomposition within sediments to sediment-associated respiration. This leads to an open question and the focus of our study: To what degree are point-scale rates of organic-matter decomposition within sediments linked to reach-scale respiration associated with the whole-stream ecosystem (ER_{tot}), the sediments (ER_{sed}), or the water column (ER_{wc})? ER_{tot} represents reach scale aerobic respiration from autotrophs and heterotrophs across benthic, planktonic, and hyporheic zones. ER_{sed} comprises reach scale sediment-associated respiration from benthic/streambed sediments, rooted/submerged plants, and hyporheic zones that are hydrologically connected to the active channel, and ER_{wc} constitutes reach scale planktonic respiration occurring only in the water column.

We specifically tested the hypothesis that reach-scale ER_{sed} rates are strongly linked to point-scale measurements of organic matter decomposition within streambed sediments. More specifically, we tested the prediction that cotton-strip-decay rates will be best explained by ER_{sed} , with little additional variation in decay rates explained by ER_{tot} or ER_{wc} . To test our hypothesis and associated prediction we used field deployments across the Yakima River Basin (YRB). The YRB is an environmentally diverse basin in southeastern Washington State (USA) that is $\sim 16,000 \text{ km}^2$ and with a stream network that culminates in the 7th-order Yakima River. To generate the data needed to test our hypothesis, we used a combination of sensors and cotton strips across 48 sites in the YRB that collectively spanned a



81 continuum from small mountainous streams in coniferous forests with little human impact to a large
 82 lowland river in an arid environment surrounded by significant agricultural land use. The resulting
 83 patterns help to fill a fundamental knowledge gap in our understanding of how organic matter
 84 decomposition relates to respiration and can be used to inform models that aim to mechanistically
 85 integrate biogeochemical processes within and across stream networks.

86

87 **Methods**

88 To evaluate the linkages between organic matter decomposition and stream ecosystem respiration we
 89 took advantage of a prior study (Garayburu-Caruso et al., 2025) that separated ER_{tot} , ER_{sed} , and ER_{wc}
 90 across environmentally divergent locations in the YRB (Fig. 1). Garayburu-Caruso et al. (2025) used
 91 dissolved oxygen (DO) sensors, dark bottle incubations, and the single-station method (Odum, 1956) to
 92 estimate these three components of respiration. In addition, that study deployed sensors to log water
 93 temperature used here to calculate cumulative degree days, as described below. These and associated
 94 contextual data were downloaded from existing data packages (Delgado et al., 2023; Forbes et al., 2023;
 95 Garayburu-Caruso et al., 2023), and methods are described in detail by Garayburu-Caruso et al. (2025).
 96 In brief, DO timeseries were analyzed via StreamMetabolizer (Appling et al., 2018) to estimate ER_{tot} . To
 97 estimate ER_{wc} , 2 L opaque bottles containing a DO sensor were filled with stream water and incubated *in*
 98 *situ*; the rate of DO drawdown was used as the estimate of ER_{wc} . The difference between ER_{tot} and ER_{wc}
 99 was used as an estimate of ER_{sed} , which represents all respiration in the stream system that is not
 100 directly occurring in the water column. ER_{sed} therefore includes respiration in the hyporheic zone, the
 101 streambed surface, and rooted/submerged plants.

102 To take advantage of the ecosystem respiration study, cotton strips made of Artist fabric (following the
 103 protocol of Tiegs et al., 2013) were deployed at the same time as the DO sensors. They were deployed
 104 upstream of the DO sensors to capture the upstream reach that influenced the DO sensor readings and
 105 prevent disturbance during sensor maintenance.

106 The cotton strips were deployed at the interface between water and sediments for 35 continuous days
 107 at 48 sites across the YRB (Fig. 1). Deployment and retrieval days varied across four days, but all strips
 108 were deployed for 35 days: deployments were from July 25th to July 28th, 2022 and retrievals were from
 109 August 29th to September 1st, 2022. Cotton strips were cut from bolts of 12-ounce, heavy-weight cotton
 110 fabric composed of 95% cellulose (Style 548; Fredrix, Lawrenceville, GA, USA). Each strip was 27 threads
 111 wide and cut to 8.0 cm by 2.5 cm. Each cotton strip was laid flat in a stainless-steel mesh cage (10.8 x 4.5
 112 cm, RSV Jumbo Mesh Herb Infuser) to minimize physical damage and feeding by macroinvertebrates,
 113 thereby emphasizing microbe-based decomposition. At each site, four cages with one strip each were
 114 attached to the underside of clay bricks (20 x 10 x 5.5 cm) with stainless steel wire. The brick/cage/strip
 115 setup was nestled into streambed sediment such that the cages/strips were within the sediments and
 116 the brick was at the sediment/water interface. The four cages were next to each other. This setup kept
 117 the cotton strips out of direct light and within the sediments while allowing water to flow past the
 118 cotton strips.

119 After the 35-day incubation period, cotton strips were carefully removed from cages and gently brushed
 120 with gloved hands in stream water for approximately 10 s to remove large debris. Cleaned cotton strips
 121 were placed in 50 mL conical centrifuge tubes with 70% ethanol. Tubes were capped and rolled



approximately 10 times before ethanol was removed, and clean 70% ethanol was added to the 50 mL tube to minimize further microbial-based decomposition. Cotton strips were transported in the ethanol filled tubes on blue ice to Pacific Northwest National Laboratory in Richland, WA. At the laboratory, the ethanol was removed from the tubes and cotton strips were air dried overnight prior to further drying in an oven at 40 °C for at least 24 hours. After drying, cotton strips were stored in air-tight containers with desiccant.

Dried cotton strips were shipped to Oakland University for tensile strength analysis following the protocol in Tiegs et al., (2013). A tensiometer was used to estimate tensile strength (Mark 10 MG100 with a Chatillon TCM 201 with roller jaws). The tensiometer pulled each cotton strip at a rate of 2 cm/min. Some of the cotton strips were completely degraded such that there was no material to measure, while other cages only contained fragments that were too small to measure tensile strength. In both cases, a limit of detection was assigned as the lowest tensile strength calculated in Tiegs et al. (2019) divided by 2, resulting in a final value of 0.05. This was done to avoid statistical artifacts that can arise when simply introducing a value of 0.

Tensiometer data were converted into decay rates using tensile loss calculated via Equation 1 (as in Mancuso et al., 2022).

$$K = \frac{-\ln(T_s/T_{sc})}{Time} \quad \text{Equation 1}$$

Here, K is the decomposition rate, T_s is the post-incubation tensile strength of the deployed cotton strips, and T_{sc} is the mean tensile strength of control strips that were not incubated in the field. The time variable was calculated as either the number of chronological deployment days (i.e., 35 days) or the number of degree days. Using degree days as the time variable accounts for variation in temperature across field sites and was estimated separately for each site as the sum of mean daily river temperature over the incubation period. We use K_{cd} and K_{dd} to represent decay rate per chronological day or per degree day, respectively. The values of K_{cd} and K_{dd} were estimated for each individual cotton strip and then replicates were averaged to provide a single site-level value for K_{cd} and K_{dd} .

We examined both K_{cd} and K_{dd} to evaluate whether the connection between decomposition and reach-scale respiration rates depends on accounting for temperature variation across the study basin. This is particularly relevant in the YRB because our field sites ranged from colder headwater streams to warmer low-gradient rivers. To test our hypothesis, we conducted both univariate and multivariate regression-based analyses. We used ordinary least squares regression to examine the strength of univariate correlations between K_{cd} or K_{dd} and ER_{tot} , ER_{wcr} , or ER_{sed} . We complemented this univariate analysis with multiple regression analysis to find an optimized model to explain variation in either K_{cd} or K_{dd} .

Further, to explore how other system variables may explain further variation in decomposition rates, a LASSO (Least Absolute Shrinkage and Selection Operator) regression model was built using physical, chemical and environmental variables (Table S1) as inputs, and K_{cd} or K_{dd} as the response variables. Variables were cube root transformed and z-score normalized to reduce the impact of high leverage points in the regression analysis and to equally weight all variables. The LASSO regression was performed over 100 iterations, each with a different random seed using the `cv.glmnet` function in the `glmnet` R package (Friedman et al., 2010). β coefficients were normalized to the maximum β coefficient for each iteration, then averaged over the 100 iterations for the final reported value. Both the raw and normalized mean β coefficient and standard deviation are reported in addition to the R^2 (Table 2).



163

164 **Results and Discussion**

165 **Decomposition in the Yakima River Basin spans globally reported rates**

166 Both K_{cd} and K_{dd} exhibited a wide range of values (Fig. 2), effectively spanning the theoretical maximum
 167 of what could have been observed with our deployment setup. This is evidenced by some cotton strips
 168 being completely consumed prior to retrieval (K_{cd} and K_{dd} maximized), while others were largely intact
 169 (K_{cd} and $K_{dd} \approx 0$). This variation is surprising given the relatively small spatial domain sampled by this
 170 study, and emphasizes that environmental heterogeneity can surpass the effects of spatial extent
 171 (Mancuso et al., 2022). The environments studied here ranged from pristine locations in the
 172 mountainous headwaters of the YRB to lowland locations with heavy agricultural influences (Fig. 1; Laan
 173 et al. 2025). This emphasizes the value of climatically diverse watersheds like the YRB as useful testbeds
 174 to study variation in decomposition rates within single hydrologically connected basins.

175 Comparing decay rates from the YRB to a global dataset from > 500 streams and rivers (Tiegs et al.,
 176 2024) showed that YRB rates spanned nearly the entire global range and had substantial overlap with
 177 the bulk of the global distributions (Fig. 2a,b). Dominant peaks in the YRB rate distributions were shifted
 178 slightly towards faster rates, relative to primary peaks in the global dataset (Fig. 2a,b). This shift towards
 179 faster rates and the wide range in rates may be because YRB rates were estimated in later summer, a
 180 time of year when decay processes are likely maximized due to relatively high temperatures and slow
 181 flows (Collier et al., 2013b; Mancuso et al., 2023). The two decay rates were also closely correlated with
 182 each other, though the relationship weakened towards locations with faster decay rates (Fig. 2c). This
 183 suggests a weak influence of temperature in the YRB; a strong influence of temperature should lead to a
 184 weak relationship between K_{cd} and K_{dd} . These results are surprising given previously reported influences
 185 of temperature on particulate organic matter decomposition (Benbi et al., 2014; Griffiths and Tiegs,
 186 2016). Temperature-driven decomposition is also expected to lead to a strong relationship between K_{cd}
 187 and summed temperature, but we observed a very weak relationship despite ~4-fold variation in
 188 summed temperature (Fig. 2d). This range in temperature among sites would likely be smaller in other
 189 seasons, and we do not therefore expect a strong influence of temperature to emerge in the YRB by
 190 conducting the study in other seasons. These results emphasize the need to understand factors
 191 governing variation in decay rates across the YRB. This is especially true given that rate distributions
 192 within this one basin span nearly all globally observed decay rates.

193 Across the YRB there appears to be potential for some spatial organization for both K_{cd} and K_{dd} (Fig. 3).
 194 Visual inspection of the maps suggests that the spatial organization may be stronger for K_{cd} than for K_{dd} .
 195 To evaluate this possibility more rigorously, we regressed each decay rate against upstream drainage
 196 area (Fig. 4). In this case, drainage area is meant to reflect position within the YRB. We used drainage
 197 area in preference to stream order because it is a continuous variable directly tied to the spatial domain
 198 a given stream integrates, whereas stream order is categorical and primarily reflects stream network
 199 topology. Associated regressions were significant ($p < 0.05$) with both decay rates increasing with
 200 drainage area (Fig. 4). The relationship with drainage area was stronger, in terms of R^2 , for K_{cd} . Both
 201 relationships were, however, relatively weak with R^2 values of 0.22 and 0.14 for K_{cd} and K_{dd} , respectively
 202 (Fig. 4). Nonetheless, the existence of a significant relationship after controlling for temperature (i.e., for
 203 K_{dd}) indicates that spatially structured factors other than temperature influence decay rates. This is not
 204 surprising as studies using cotton strips have found several factors that influence decomposition, such as



205 nutrient concentrations, turbidity, and many others (Collier et al., 2013b; Pingram et al., 2020; Tiegs et
 206 al., 2024). Before exploring a broad suite of potential explanatory variables, we tested our hypothesis
 207 that decomposition rates will be better explained by sediment-associated respiration (ER_{sed}) than by
 208 respiration in the water column (ER_{wc}) or by respiration of the integrated stream system (ER_{tot}).

209

210 **Respiration in sediments explains little variation in decomposition**

211 Contrary to our hypothesis, we found that both decay rates were most strongly connected to ER_{tot} , less
 212 so with ER_{sed} , and not at all with ER_{wc} (**Fig. 5**). Univariate models using ER_{tot} were better than multivariate
 213 models using ER_{sed} , ER_{wc} , and their interaction. This is evidenced by univariate models using ER_{tot} having
 214 AIC values more than two units lower than multivariate models containing ER_{sed} and ER_{wc} (**Table 1**).
 215 Multivariate models were not used with ER_{tot} because it contains ER_{sed} and ER_{wc} . These results are
 216 surprising, in part, because the cotton strips were deployed within the shallow hyporheic zones (i.e.,
 217 within the riverbed sediments). This deployment strategy is a key reason we hypothesized that decay
 218 rates would be most strongly connected to ER_{sed} . The results indicate that decomposition of particulate
 219 organic matter within the shallow hyporheic zone is linked to respiratory processes occurring in both the
 220 sediment and water column. We propose that if our deployment configuration was complemented with
 221 a simultaneous deployment that enabled growth of benthic algal biofilms on the cotton strips, the
 222 combined decomposition from both deployments would capture substantially more of the processes
 223 that contribute to ER_{sed} . This would provide a more complete view of sediment-associated
 224 biogeochemical function, potentially leading to a stronger correlation between decomposition rates and
 225 ER_{sed} . While this remains to be tested, the underlying idea is that primary producers support a large
 226 portion of heterotrophic respiration associated with riverbed sediments, which is supported by recent
 227 analyses showing a strong link between ER_{sed} and gross primary production across the YRB (Garayburu-
 228 Caruso et al., 2025).

229

230 **Slower rates of K_{cd} and K_{dd} are in streams with coarse sediments, set within wet forests**

231 Given that our hypothesis was rejected and that ER_{tot} explained only about 29% and 16% of K_{cd} and K_{dd} ,
 232 respectively (**Table 1, Figure 5**), we used a discovery-based approach to explore other system variables
 233 that may explain further variation in decomposition rates. LASSO-based modeling indicated that total
 234 dissolved nitrogen (TDN) and the median grain size of sediment texture (D50) were most important for
 235 explaining K_{dd} , while TDN and aridity were most important for explaining K_{cd} (**Table 2**). Other variables
 236 were retained in the LASSO models (**Table S1**), but we interpreted TDN, D50, and aridity as the most
 237 important because they consistently had the largest normalized coefficients. This interpretation is based
 238 on these variables having mean normalized coefficients above 0.5—in terms of absolute value—
 239 meaning they were at least 50% as important as the most important variable in the 100 LASSO model
 240 runs. Further, the LASSO coefficients for these variables had a coefficient of variation less than 0.5,
 241 meaning that across the 100 LASSO model runs the values of their normalized coefficients were
 242 relatively stable (**Table S1**). The LASSO modeling also confirmed a relatively weak influence of
 243 temperature, evidenced by relatively small and highly variable β coefficients for summed temperature in
 244 the K_{cd} model (**Table S1**); temperature was not used in the K_{dd} model.



Both decomposition rates increased with higher TDN concentrations, while Kdd decreased with larger D50 and Kcd decreased with higher aridity index values (**Table 1**). To more deeply interpret these relationships, we examined Pearson-based univariate correlations between these three explanatory variables and other variables included in the LASSO models. This is important because of strong collinearity among some explanatory variables (**Fig. S1**). In this case, variables identified as being the most important may be acting as proxies for one or more additional variables. We found that TDN was most strongly correlated with percent agricultural land cover of the upstream drainage area and sulfate concentrations in the stream water (**Fig. S1**). Increases in both decomposition rates with TDN may, therefore, reflect agricultural inputs of nutrients that increase overall microbial activity of the stream ecosystems we studied. D50 was most strongly correlated with the aridity index, which was most strongly correlated with percent forest cover; the correlation between D50 and aridity is unlikely to reflect a causal connection, while aridity and forest cover most likely are causally linked. If the relationship between decomposition and D50 is causal, it could be mediated by the total surface area available for microbial attachment. Coarser sediments have much less surface area, potentially limiting overall microbial activity.

Considering the directionality of the univariate relationships, in context of the LASSO outcomes, suggests slower decomposition—for both rates—in streams with relatively coarse sediments and set within relatively wet forests. This contrasts with Clapcott and Barmuta (2010) who found faster decomposition in coarser sediments. The discrepancy is likely because we excluded macroinvertebrates while they did not, and they interpreted the link to sediment texture as due to greater habitat availability for macroinvertebrates in coarser sediments. Locations with slower decomposition should, thus, primarily be in higher elevation, relatively pristine parts of the YRB, while faster decomposition occurs at lower elevations impacted by agricultural inputs. These results are consistent with previous work showing greater cotton strip decomposition in impaired streams (Young and Collier, 2009), those with little natural land cover (Collier et al., 2013a; Webb et al., 2019), and in streams with higher nutrient concentrations (Ferreira et al., 2015; Pingram et al., 2020; Tiegs et al., 2013). In addition to differences in nutrient concentrations between higher and lower elevation sites, we expect less light penetration to streams in higher elevation sites because of more forest cover and smaller streams. Though not measured here, less light could suppress autotrophic production which will limit heterotrophic respiration (Bernhardt et al., 2022; Mulholland et al., 2001; Young and Huryn, 1999) and, in turn, indirectly lead to slower decomposition.

276

277 **Decomposition is linked to processes across the sediment-water continuum and land features**

Our results collectively indicate that to study shallow hyporheic zone decomposition processes, it is not sufficient to conceptualize organic-matter decomposition by only considering sediment or water column processes; one must examine the integrated system. The implication of our analyses is that organic matter decomposition rates are linked to the integrated system more strongly than they are linked to individual components or direct interactions between components of that integrated system. Mechanistic models of stream ecosystem respiration, therefore, need to account for sediment processes, water-column processes, and land-cover influences from beyond the stream. Focusing exclusively on the hyporheic zone is insufficient, even in systems for which the hyporheic zone accounts for most reactions (Boano et al., 2014; Burrows et al., 2017; McClain et al., 2003). This is further



emphasized by previous work showing that most respiration occurs in the water column of large rivers (Gardner and Doyle, 2018; Roley et al., 2023). Garayburu-Caruso et al. (2025) also show that fractional contributions of ER_{sed} to ER_{tot} is often high, but that there is significant variation in those fractional influences across the YRB. This variability is due to ER_{wc} being fast enough, in some locations, to account for more than 80% of ER_{tot} (Garayburu-Caruso et al., 2025). Similarly, Laan et al. (2025) found substantial overlap between the distribution of ER_{wc} rates from the YRB and ER_{tot} from across the contiguous United States. The overall picture is that decomposition is the result of integrated processes occurring across the sediment-water continuum and influenced by external factors tied to land cover and land use. We infer that these integrated processes are influenced by biophysical variation across the YRB (Laan et al., 2025), leading to decomposition rates within this single basin that resemble global rate distributions and nearly span the global range of observed rates (Tiegs et al., 2024). Other basins that contain only one ecoregion or have homogeneous land cover may be expected to have a narrow range of decomposition rates (Webb et al., 2019). Nonetheless, models applied to any stream network that aim to predict spatiotemporal variation in decomposition rates would be well served by considering processes throughout the integrated watershed system.

Code and data availability

Data and scripts used to generate the main findings within this manuscript can be found at <https://github.com/river-corridors-sfa/rcsfa-ST-2B-SSS-cotton-strip>. Upon acceptance of this manuscript, they will be published on the U.S. Department of Energy's Environmental System Science Data Infrastructure for a Virtual Ecosystem (ESS-DIVE) repository. Other data collected during the field efforts (i.e., sensor data; surface water chemistry data; and geospatial information, metadata, and maps for 2021 Spatial Study sampling event) can be accessed on ESS-DIVE at <https://data.ess-dive.lbl.gov/datasets/doi:10.15485/1987520> (Garayburu-Caruso et al., 2023), <https://data.ess-dive.lbl.gov/datasets/doi:10.15485/1969566> (Delgado et al., 2023), and <https://data.ess-dive.lbl.gov/datasets/doi:10.15485/1923689> (Forbes et al., 2023).

Author contributions

Conceptualization: JCS, MB, VAGC, PR, ST
 Data Curation: MB, JCS, BF, ML, SM, DD, LR and AEG
 Formal Analysis: MB, MML, BF, and JCS
 Funding Acquisition: JCS
 Investigation: MB, DD, BF, VAGC, AEG, ML, SM, PR, LR, ST and JCS
 Methodology: MB, DD, BF, VAGC, AEG, ML, SM, PR, LR, ST and JCS
 Project Administration: MB, VAGC and JCS
 Resources: MB, DD, BF, VAGC, AEG, ML, SM, PR, LR, ST and JCS
 Software: MB, MML, BF, and JCS
 Supervision: MB, VAGC and JCS
 Validation: MB and JCS



324 Visualization: MB, MML, BF, and JCS
 325 Writing – Original Draft Preparation: MB, VAGC, ST and JCS
 326 Writing – Review & Editing: MB, DD, BF, VAGC, AEG, ML, SM. PR, LR, ST and JCS

327 **Competing interest**

328 The authors declare that they have no conflict of interest.

329 **Acknowledgements**

330 This work was supported by the River Corridor Science Focus Area (RC-SFA) at the Pacific Northwest
 331 National Laboratory (PNNL). The RC-SFA is supported by the United States Department of Energy, Office
 332 of Biological and Environmental Research (BER), Environmental System Science (ESS) Program. PNNL is
 333 operated by Battelle Memorial Institute for the United States Department of Energy under contract no.
 334 DE-AC05-76RL01830. We thank the United States Forest Service, Washington Department of Natural
 335 Resources, Washington Department of Fish and Wildlife, Confederated Tribes and Bands of the Yakama
 336 Nation, and Cowlitz Canyon Conservancy for access to field locations where these samples were
 337 collected. We also thank the Confederated Tribes and Bands of the Yakama Nation Tribal Council and
 338 Yakama Nation Fisheries for working with us to facilitate sample collection and optimization of data
 339 usage according to their values and worldview. We thank the field team including: Dillman Delgado,
 340 Morgan Barnes, Brandon T. Boehnke, Yunxiang Chen, Kali Cornwell, Brianna I. Gonzalez, Samantha
 341 Grieger, Glenn E. Hammond, Peishi Jiang, Bing Li, Zhi Li, Xinming Lin, Sophia A. McKeever, Maruti K.
 342 Mudunuru, Katherine A. Muller, Opal Otenburg, Aaron Pelly, Kelsey Peta, Alan Roebuck, Joshua M.
 343 Torgeson, and Jianqiu Zheng.

345 **References**

- 346 Allan, J. D., Castillo, M. M., and Capps, K. A.: Stream Ecology: Structure and Function of Running Waters,
 347 Springer International Publishing, Cham, <https://doi.org/10.1007/978-3-030-61286-3>, 2021.
- 348 Appling, A. P., Hall Jr., R. O., Yackulic, C. B., and Arroita, M.: Overcoming Equifinality: Leveraging Long
 349 Time Series for Stream Metabolism Estimation, *Journal of Geophysical Research: Biogeosciences*, 123,
 350 624–645, <https://doi.org/10.1002/2017JG004140>, 2018.
- 351 Battin, T. J., Lauerwald, R., Bernhardt, E. S., Bertuzzo, E., Gener, L. G., Hall, R. O., Hotchkiss, E. R.,
 352 Maavara, T., Pavelsky, T. M., Ran, L., Raymond, P., Rosentreter, J. A., and Regnier, P.: River ecosystem
 353 metabolism and carbon biogeochemistry in a changing world, *Nature*, 613, 449–459,
 354 <https://doi.org/10.1038/s41586-022-05500-8>, 2023.
- 355 Benbi, D. K., Boparai, A. K., and Brar, K.: Decomposition of particulate organic matter is more sensitive to
 356 temperature than the mineral associated organic matter, *Soil Biology and Biochemistry*, 70, 183–192,
 357 <https://doi.org/10.1016/j.soilbio.2013.12.032>, 2014.
- 358 Benfield, E. F., Fritz, K. M., and Tiegs, S. D.: Chapter 27 - Leaf-Litter Breakdown, in: *Methods in Stream*
 359 *Ecology (Third Edition)*, edited by: Lamberti, G. A. and Hauer, F. R., Academic Press, 71–82,
 360 <https://doi.org/10.1016/B978-0-12-813047-6.00005-X>, 2017.



- 361 Bernhardt, E. S., Savoy, P., Vlah, M. J., Appling, A. P., Koenig, L. E., Hall, R. O., Arroita, M., Blaszcak, J. R.,
 362 Carter, A. M., Cohen, M., Harvey, J. W., Heffernan, J. B., Helton, A. M., Hosen, J. D., Kirk, L., McDowell,
 363 W. H., Stanley, E. H., Yackulic, C. B., and Grimm, N. B.: Light and flow regimes regulate the metabolism of
 364 rivers, *Proceedings of the National Academy of Sciences*, 119, e2121976119,
 365 <https://doi.org/10.1073/pnas.2121976119>, 2022.
- 366 Boano, F., Harvey, J. W., Marion, A., Packman, A. I., Revelli, R., Ridolfi, L., and Wörman, A.: Hyporheic
 367 flow and transport processes: Mechanisms, models, and biogeochemical implications, *Reviews of*
 368 *Geophysics*, 52, 603–679, <https://doi.org/10.1002/2012RG000417>, 2014.
- 369 Boulton, A. J., Findlay, S., Marmonier, P., Stanley, E. H., and Valett, H. M.: The functional significance of
 370 the hyporheic zone in streams and rivers, *Annual Review of Ecology, Evolution, and Systematics*, 29, 59–
 371 81, <https://doi.org/10.1146/annurev.ecolsys.29.1.59>, 1998.
- 372 Burrows, R. M., Rutledge, H., Bond, N. R., Eberhard, S. M., Auhl, A., Andersen, M. S., Valdez, D. G., and
 373 Kennard, M. J.: High rates of organic carbon processing in the hyporheic zone of intermittent streams,
 374 *Sci Rep*, 7, 13198, <https://doi.org/10.1038/s41598-017-12957-5>, 2017.
- 375 Clapcott, J. E. and Barmuta, L. A.: Metabolic patch dynamics in small headwater streams: exploring
 376 spatial and temporal variability in benthic processes, *Freshwater Biology*, 55, 806–824,
 377 <https://doi.org/10.1111/j.1365-2427.2009.02324.x>, 2010.
- 378 Colas, F., Woodward, G., Burdon, F. J., Guérol, F., Chauvet, E., Cornut, J., Cébron, A., Clivot, H., Danger,
 379 M., Danner, M. C., Pagnout, C., and Tiegs, S. D.: Towards a simple global-standard bioassay for a key
 380 ecosystem process: organic-matter decomposition using cotton strips, *Ecological Indicators*, 106,
 381 105466, <https://doi.org/10.1016/j.ecolind.2019.105466>, 2019.
- 382 Cole, J. J., Prairie, Y. T., Caraco, N. F., McDowell, W. H., Tranvik, L. J., Striegl, R. G., Duarte, C. M.,
 383 Kortelainen, P., Downing, J. A., Middelburg, J. J., and Melack, J.: Plumbing the Global Carbon Cycle:
 384 Integrating Inland Waters into the Terrestrial Carbon Budget, *Ecosystems*, 10, 172–185,
 385 <https://doi.org/10.1007/s10021-006-9013-8>, 2007.
- 386 Collier, K. J., Clapcott, J. E., Hamer, M. P., and Young, R. G.: Extent estimates and land cover relationships
 387 for functional indicators in non-wadeable rivers, *Ecological Indicators*, 34, 53–59,
 388 <https://doi.org/10.1016/j.ecolind.2013.04.010>, 2013a.
- 389 Collier, K. J., Clapcott, J. E., Duggan, I. C., Hamilton, D. P., Hamer, M., and Young, R. G.: Spatial Variation
 390 of Structural and Functional Indicators in a Large New Zealand River, *River Research and Applications*,
 391 29, 1277–1290, <https://doi.org/10.1002/rra.2609>, 2013b.
- 392 Delgado, D., Barnes, M., Boehnke, B. T., Chen, X., Chen, Y., Cornwell, K., Forbes, B., Fulton, S. G.,
 393 Garayburu-Caruso, V. A., Goldman, A. E., Gonzalez, B. I., Grieger, S., Hammond, G. E., Jiang, P., Kaufman,
 394 M. H., Laan, M., Li, B., Li, Z., Lin, X., McKeever, S. A., Mudunuru, M. K., Muller, K. A., Myers-Pigg, A.,
 395 Otenburg, O., Pelly, A., Peta, K., Powers-McCormack, B., Regier, P., Renteria, L., Roebuck, A., Scheibe, T.
 396 D., Son, K., Torgeson, J. M., Zheng, J., and Stegen, J. C.: Spatial Study 2022: Surface Water Samples,
 397 Cotton Strip Degradation, and Hydrologic Sensor Data across the Yakima River Basin, Washington, USA
 398 (v3), 2023.



- 399 Drake, T. W., Raymond, P. A., and Spencer, R. G. M.: Terrestrial carbon inputs to inland waters: A current
400 synthesis of estimates and uncertainty, *Limnology and Oceanography Letters*, 3, 132–142,
401 <https://doi.org/10.1002/lol2.10055>, 2018.
- 402 Fellows, C. S., Valett, M. H., and Dahm, C. N.: Whole†stream metabolism in two montane streams:
403 Contribution of the hyporheic zone, *Limnology and Oceanography*, 46, 523–531,
404 <https://doi.org/10.4319/lo.2001.46.3.0523>, 2001.
- 405 Ferreira, V., Castagnyrol, B., Koricheva, J., Gulis, V., Chauvet, E., and Graça, M. A. S.: A meta-analysis of
406 the effects of nutrient enrichment on litter decomposition in streams, *Biological Reviews*, 90, 669–688,
407 <https://doi.org/10.1111/brv.12125>, 2015.
- 408 Filbee-Dexter, K., Feehan, C. J., Smale, D. A., Krumhansl, K. A., Augustine, S., Bettignies, F. de, Burrows,
409 M. T., Byrnes, J. E. K., Campbell, J., Davoult, D., Dunton, K. H., Franco, J. N., Garrido, I., Grace, S. P.,
410 Hancke, K., Johnson, L. E., Konar, B., Moore, P. J., Norderhaug, K. M., O'Dell, A., Pedersen, M. F.,
411 Salomon, A. K., Sousa-Pinto, I., Tiegs, S., Yiu, D., and Wernberg, T.: Kelp carbon sink potential decreases
412 with warming due to accelerating decomposition, *PLOS Biology*, 20, e3001702,
413 <https://doi.org/10.1371/journal.pbio.3001702>, 2022.
- 414 Forbes, B., Barnes, M., Boehnke, B. T., Bowden, M. E., Chen, X., Cornwell, K., Crawford, M., Delgado, D.,
415 Fulton, S. G., Garayburu-Caruso, V. A., Gary, S., Goldman, A. E., Gonzalez, B. I., Grieger, S., Hammond, G.
416 E., Jiang, P., Kaufman, M. H., Laan, M., Li, B., Li, Z., McKeever, S. A., Mudunuru, M. K., Muller, K. A., Myers-
417 Pigg, A., Ocejo, J. A., Otenburg, O., Pelly, A., Peta, K., Powers-McCormack, B., Regier, P., Renteria, L.,
418 Roebuck, A., Scheibe, T. D., Son, K., Tfaily, M. M., Torgeson, J. M., Stegen, J. C., and Consortium, T. W.:
419 WHONDRS River Corridor Sediment and Water Geochemistry and In Situ Sensor Data from Machine-
420 Learning-Informed Sites across the Contiguous United States (v6), 2023.
- 421 Friedman, J., Hastie, T., and Tibshirani, R.: Regularization Paths for Generalized Linear Models via
422 Coordinate Descent, *Journal of Statistical Software*, 33, 1–22, <https://doi.org/10.18637/jss.v033.i01>,
423 2010.
- 424 Garayburu-Caruso, V. A., Kaufman, M. H., Delgado, D., Barnes, M., Boehnke, B. T., Chen, X., Cornwell, K.,
425 Forbes, B., Fulton, S. G., Goldman, A. E., Gonzalez, B. I., Grieger, S., Jr, R. O. H., Hammond, G. E., Jiang, P.,
426 Laan, M., Li, B., Li, Z., Lin, X., McKeever, S. A., Mudunuru, M. K., Muller, K. A., Myers-Pigg, A., Otenburg,
427 O., Pelly, A., Peta, K., Regier, P., Renteria, L., Roebuck, A., Scheibe, T. D., Son, K., Torgeson, J. M., and
428 Stegen, J. C.: Spatial Study 2022: Water Column, Sediment, and Total Ecosystem Respiration Rates across
429 the Yakima River Basin, Washington, USA (v2), 2023.
- 430 Garayburu-Caruso, V. A., Kaufman, M., Forbes, B., Hall, R. O., Laan, M., Chen, X., Lin, X., Fulton, S.,
431 Renteria, L., Fang, Y., Son, K., and Stegen, J. C.: Sediment-associated processes account for most of the
432 spatial variation in ecosystem respiration in the Yakima River basin, *bioRxiv*, 2024.03.22.586339,
433 <https://doi.org/10.1101/2024.03.22.586339>, 2025.
- 434 Gardner, J. R. and Doyle, M. W.: Sediment–Water Surface Area Along Rivers: Water Column Versus
435 Benthic, *Ecosystems*, 21, 1505–1520, <https://doi.org/10.1007/s10021-018-0236-2>, 2018.
- 436 Griffiths, N. A. and Tiegs, S. D.: Organic-matter decomposition along a temperature gradient in a
437 forested headwater stream, *Freshwater Science*, 35, 518–533, 2016.



- 438 Hall, R. O. and Hotchkiss, E. R.: Chapter 34 - Stream Metabolism, in: *Methods in Stream Ecology* (Third
439 Edition), edited by: Lamberti, G. A. and Hauer, F. R., Academic Press, 219–233,
440 <https://doi.org/10.1016/B978-0-12-813047-6.00012-7>, 2017.
- 441 Krause, S., Hannah, D. M., Fleckenstein, J. H., Heppell, C. M., Kaeser, D., Pickup, R., Pinay, G., Robertson,
442 A. L., and Wood, P. J.: Inter-disciplinary perspectives on processes in the hyporheic zone, *Ecohydrology*,
443 4, 481–499, <https://doi.org/10.1002/eco.176>, 2011.
- 444 Laan, M. M., Fulton, S. G., Garayburu-Caruso, V. A., Barnes, M. E., Borton, M. A., Chen, X., Farris, Y.,
445 Forbes, B., Goldman, A. E., Grieger, S., Hall Jr., R. O., Kaufman, M. H., Lin, X., Zionce, E. L. M., McKeever, S.
446 A., Myers-Pigg, A., Otenburg, O., Pelly, A. C., Ren, H., Renteria, L., Scheibe, T. D., Son, K., Tagestad, J.,
447 Torgeson, J. M., and Stegen, J. C.: Water column respiration in the Yakima River basin is explained by
448 temperature, nutrients, and suspended solids, *Biogeosciences*, 22, 6137–6152,
449 <https://doi.org/10.5194/bg-22-6137-2025>, 2025.
- 450 Lewandowski, J., Arnon, S., Banks, E., Batelaan, O., Betterle, A., Broecker, T., Coll, C., Drummond, J. D.,
451 Gaona Garcia, J., Galloway, J., Gomez-Velez, J., Grabowski, R. C., Herzog, S. P., Hinkelmann, R., Höhne,
452 A., Hollender, J., Horn, M. A., Jaeger, A., Krause, S., Löchner Prats, A., Magliozzi, C., Meinikmann, K.,
453 Mojarrad, B. B., Mueller, B. M., Peralta-Maraver, I., Popp, A. L., Posselt, M., Putschew, A., Radke, M.,
454 Raza, M., Riml, J., Robertson, A., Rutere, C., Schaper, J. L., Schirmer, M., Schulz, H., Shanafield, M., Singh,
455 T., Ward, A. S., Wolke, P., Wörman, A., and Wu, L.: Is the Hyporheic Zone Relevant beyond the Scientific
456 Community?, *Water*, 11, 2230, <https://doi.org/10.3390/w11112230>, 2019.
- 457 Mancuso, J., Messick, E., and Tiegs, S. D.: Parsing spatial and temporal variation in stream ecosystem
458 functioning, *Ecosphere*, 13, e4202, <https://doi.org/10.1002/ecs2.4202>, 2022.
- 459 Mancuso, J., Tank, J. L., Mahl, U. H., Vincent, A., and Tiegs, S. D.: Monthly variation in organic-matter
460 decomposition in agricultural stream and riparian ecosystems, *Aquat Sci*, 85, 83,
461 <https://doi.org/10.1007/s00027-023-00975-7>, 2023.
- 462 McClain, M. E., Boyer, E. W., Dent, C. L., Gergel, S. E., Grimm, N. B., Groffman, P. M., Hart, S. C., Harvey,
463 J. W., Johnston, C. A., Mayorga, E., McDowell, W. H., and Pinay, G.: Biogeochemical Hot Spots and Hot
464 Moments at the Interface of Terrestrial and Aquatic Ecosystems, *Ecosystems*, 6, 301–312, 2003.
- 465 Mulholland, P. J., Fellows, C. S., Tank, J. L., Grimm, N. B., Webster, J. R., Hamilton, S. K., Marti, E.,
466 Ashkenas, L., Bowden, W. B., Dodds, W. K., McDowell, W. H., Paul, M. J., and Peterson, B. J.: Inter-biome
467 comparison of factors controlling stream metabolism, *Freshwater Biology*, 46, 1503–1517,
468 <https://doi.org/10.1046/j.1365-2427.2001.00773.x>, 2001.
- 469 Naegeli, M. W. and Uehlinger, U.: Contribution of the hyporheic zone to ecosystem metabolism in a
470 prealpine gravel-bed-river, *Journal of the North American Benthological Society*, 16, 794–804, 1997.
- 471 Odum, H. T.: Primary production in flowing waters 1, *Limnology and oceanography*, 1, 102–117, 1956.
- 472 Pingram, M. A., Clapcott, J. E., Hamer, M. P., Atalah, J., and Özkundakci, D.: Exploring temporal and
473 spatial variation in cotton tensile-strength loss to assess the ecosystem health of non-wadeable rivers,
474 *Ecological Indicators*, 108, 105773, <https://doi.org/10.1016/j.ecolind.2019.105773>, 2020.



- 475 Roley, S. S., Hall Jr., R. O., Perkins, W., Garayburu-Caruso, V. A., and Stegen, J. C.: Coupled primary
 476 production and respiration in a large river contrasts with smaller rivers and streams, *Limnology and*
 477 *Oceanography*, 68, 2461–2475, <https://doi.org/10.1002/lno.12435>, 2023.
- 478 Talluto, L., del Campo, R., Estévez, E., Altermatt, F., Datry, T., and Singer, G.: Towards (better) fluvial
 479 meta-ecosystem ecology: a research perspective, *npj biodiversity*, 3, 1–10,
 480 <https://doi.org/10.1038/s44185-023-00036-0>, 2024.
- 481 Tank, J. L., Rosi-Marshall, E. J., Griffiths, N. A., Entekin, S. A., and Stephen, M. L.: A review of
 482 allochthonous organic matter dynamics and metabolism in streams, *Journal of the North American*
 483 *Benthological Society*, 29, 118–146, 2010.
- 484 Tiegs, S. D., Clapcott, J. E., Griffiths, N. A., and Boulton, A. J.: A standardized cotton-strip assay for
 485 measuring organic-matter decomposition in streams, *Ecological Indicators*, 32, 131–139,
 486 <https://doi.org/10.1016/j.ecolind.2013.03.013>, 2013.
- 487 Tiegs, S. D., Costello, D. M., Isken, M. W., Woodward, G., McIntyre, P. B., Gessner, M. O., Chauvet, E.,
 488 Griffiths, N. A., Flecker, A. S., Acuña, V., Albariño, R., Allen, D. C., Alonso, C., Andino, P., Arango, C.,
 489 Aroviita, J., Barbosa, M. V. M., Barmuta, L. A., Baxter, C. V., Bell, T. D. C., Bellinger, B., Boyero, L., Brown,
 490 L. E., Bruder, A., Bruesewitz, D. A., Burdon, F. J., Callisto, M., Canhoto, C., Capps, K. A., Castillo, M. M.,
 491 Clapcott, J., Colas, F., Colón-Gaud, C., Cornut, J., Crespo-Pérez, V., Cross, W. F., Culp, J. M., Danger, M.,
 492 Dangles, O., Eyto, E. de, Derry, A. M., Villanueva, V. D., Douglas, M. M., Elozegi, A., Encalada, A. C.,
 493 Entekin, S., Espinosa, R., Ethaiya, D., Ferreira, V., Ferriol, C., Flanagan, K. M., Fleituch, T., Shah, J. J. F.,
 494 Frainer, A., Friberg, N., Frost, P. C., Garcia, E. A., Lago, L. G., Soto, P. E. G., Ghate, S., Giling, D. P., Gilmer,
 495 A., Gonçalves, J. F., Gonzales, R. K., Graça, M. A. S., Grace, M., Grossart, H.-P., Guérol, F., Gulis, V.,
 496 Hepp, L. U., Higgins, S., Hishi, T., Huddart, J., Hudson, J., Imberger, S., Iñiguez-Armijos, C., Iwata, T.,
 497 Janetski, D. J., Jennings, E., Kirkwood, A. E., Koning, A. A., Kosten, S., Kuehn, K. A., Laudon, H., Leavitt, P.
 498 R., Silva, A. L. L. da, Leroux, S. J., LeRoy, C. J., Lisi, P. J., MacKenzie, R., Marcarelli, A. M., Masese, F. O.,
 499 McKie, B. G., Medeiros, A. O., Meissner, K., Miliša, M., Mishra, S., Miyake, Y., Moerke, A., et al.: Global
 500 patterns and drivers of ecosystem functioning in rivers and riparian zones, *Science Advances*, 5,
 501 eaav0486, <https://doi.org/10.1126/sciadv.aav0486>, 2019.
- 502 Tiegs, S. D., Capps, K. A., Costello, D. M., Schmidt, J. P., Patrick, C. J., Follstad Shah, J. J., Leroy, C. J., and
 503 CELLDEx Consortium†: Human activities shape global patterns of decomposition rates in rivers, *Science*,
 504 384, 1191–1195, 2024.
- 505 Vyšná, V., Dyer, F., Maher, W., and Norris, R.: Cotton-strip decomposition rate as a river condition
 506 indicator – Diel temperature range and deployment season and length also matter, *Ecological Indicators*,
 507 45, 508–521, <https://doi.org/10.1016/j.ecolind.2014.05.011>, 2014.
- 508 Webb, J. R., Pearce, N. J. T., Painter, K. J., and Yates, A. G.: Hierarchical variation in cellulose
 509 decomposition in least-disturbed reference streams: a multi-season study using the cotton strip assay,
 510 *Landscape Ecol*, 34, 2353–2369, <https://doi.org/10.1007/s10980-019-00893-w>, 2019.
- 511 Wondzell, S. M.: The role of the hyporheic zone across stream networks, *Hydrological Processes*, 25,
 512 3525–3532, <https://doi.org/10.1002/hyp.8119>, 2011.



- 513 Woodward, G., Gessner, M. O., Giller, P. S., Gulis, V., Hladyz, S., Lecerf, A., Malmqvist, B., McKie, B. G.,
 514 Tiegs, S. D., and Cariss, H.: Continental-scale effects of nutrient pollution on stream ecosystem
 515 functioning, *Science*, 336, 1438–1440, 2012.
- 516 Young, R. G. and Collier, K. J.: Contrasting responses to catchment modification among a range of
 517 functional and structural indicators of river ecosystem health, *Freshwater Biology*, 54, 2155–2170,
 518 <https://doi.org/10.1111/j.1365-2427.2009.02239.x>, 2009.
- 519 Young, R. G. and Huryn, A. D.: Effects of Land Use on Stream Metabolism and Organic Matter Turnover,
 520 *Ecological Applications*, 9, 1359–1376, [https://doi.org/10.1890/1051-](https://doi.org/10.1890/1051-0761(1999)009%255B1359:EOLUOS%255D2.0.CO;2)
 521 [0761\(1999\)009%255B1359:EOLUOS%255D2.0.CO;2](https://doi.org/10.1890/1051-0761(1999)009%255B1359:EOLUOS%255D2.0.CO;2), 1999.
- 522 Zarnetske, J. P., Haggerty, R., Wondzell, S. M., and Baker, M. A.: Dynamics of nitrate production and
 523 removal as a function of residence time in the hyporheic zone, *Journal of Geophysical Research:*
 524 *Biogeosciences*, 116, <https://doi.org/10.1029/2010JG001356>, 2011.

525

526

527

528

529

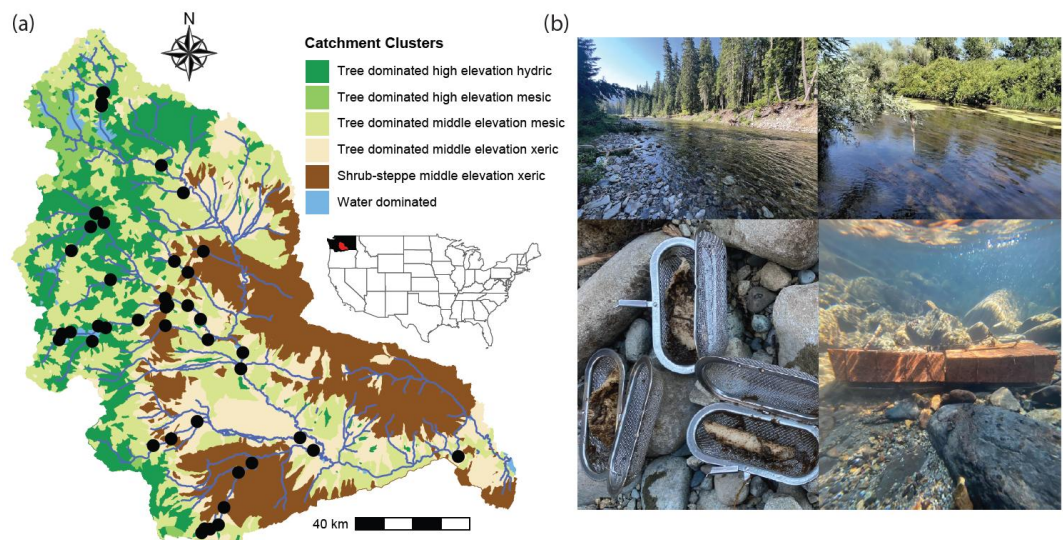
530

531

532



533 **Figures**

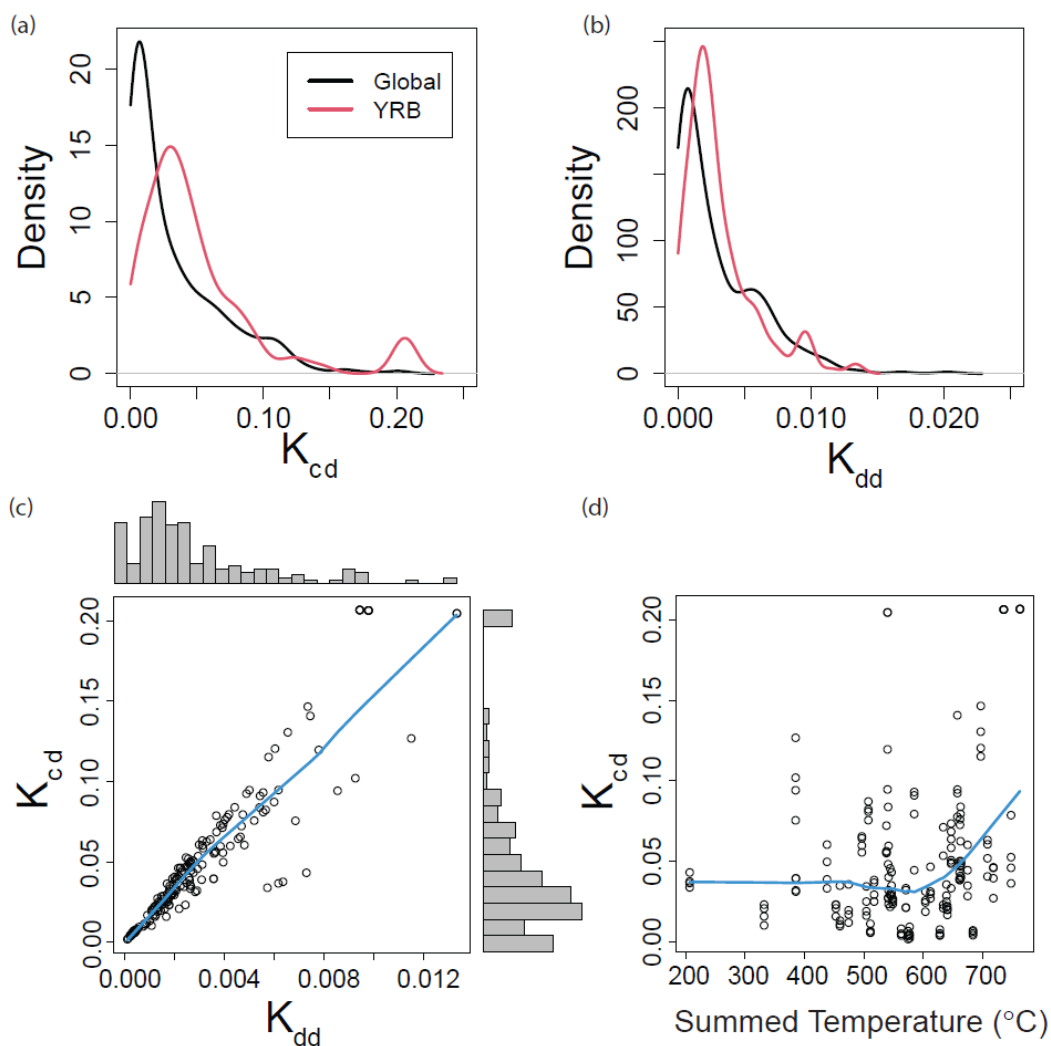


534
535 **Figure 1. Biophysical clusters, sampling locations, and example conditions across the YRB.** (a) The inset
536 map shows the location of the YRB within the contiguous United States, with black indicating
537 Washington State and red indicating the YRB. The YRB is shown with multiple colors, which correspond
538 to biophysical clusters, as presented in Laan et al. (2025) and summarized briefly in the legend. Black
539 circles are locations where decay rates were estimated. (b) Photos provide examples of the breadth of
540 conditions studied across the YRB, post-incubation states of cotton strips, and deployment of the cotton
541 strips.

542



543



544

545 **Figure 2. Decay rate distributions and relationships to each other and temperature.** Kernel density
 546 functions for (a) K_{cd} and (b) K_{dd} from a global streams/rivers dataset and from the YRB. (c) Scatterplot
 547 correlating K_{cd} to K_{dd} . Histograms summarizing the distribution of each rate are provided on the outer
 548 boundaries. (d) K_{cd} related to temperature summed across the deployment period; summed
 549 temperature was used to calculate K_{dd} . Blue lines represent lowess spline fits as regression analysis was
 550 not required for interpretation.

551

552

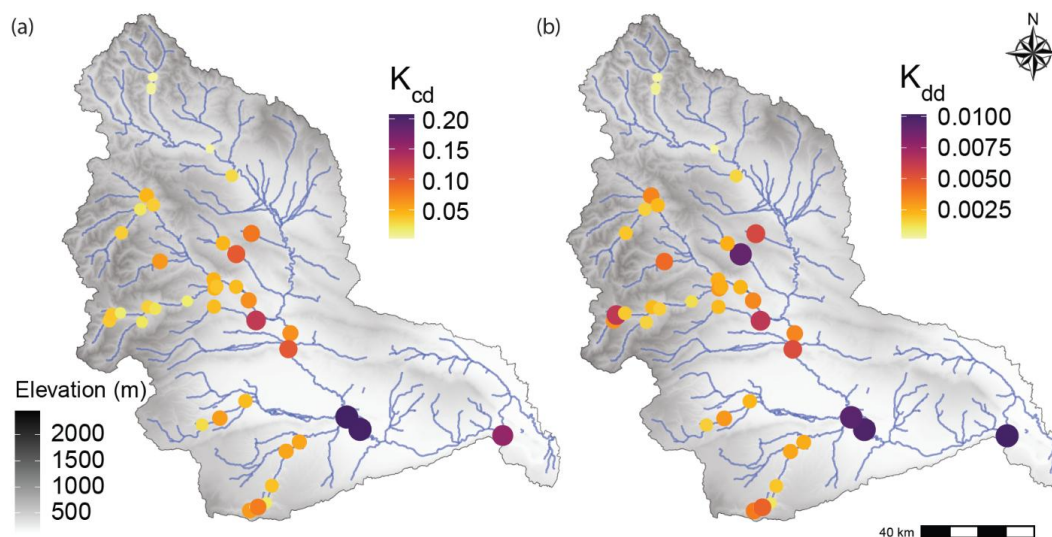
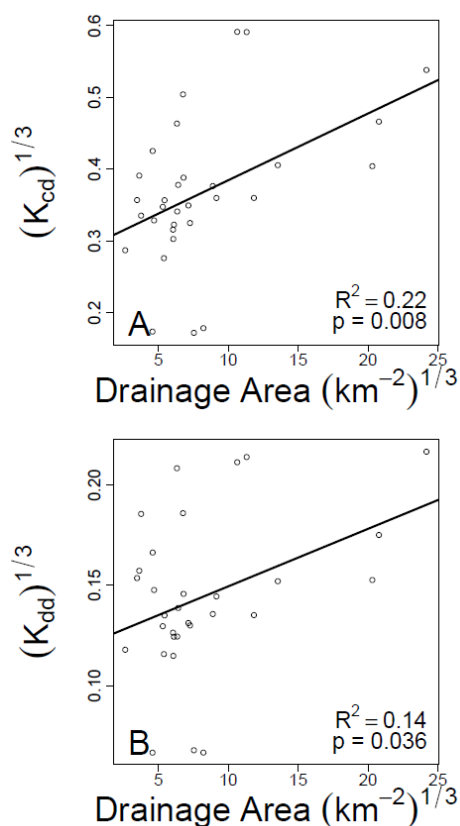


Figure 3: Spatial distribution of decay rates across the YRB. Each map shows elevation profiles and either K_{cd} (A) or K_{dd} (B). Colored circles are field locations where rates were estimated. The color of each circle is related to decay rate as indicated in the legends, and circle size is scaled to decay rate to further facilitate visual interpretability.



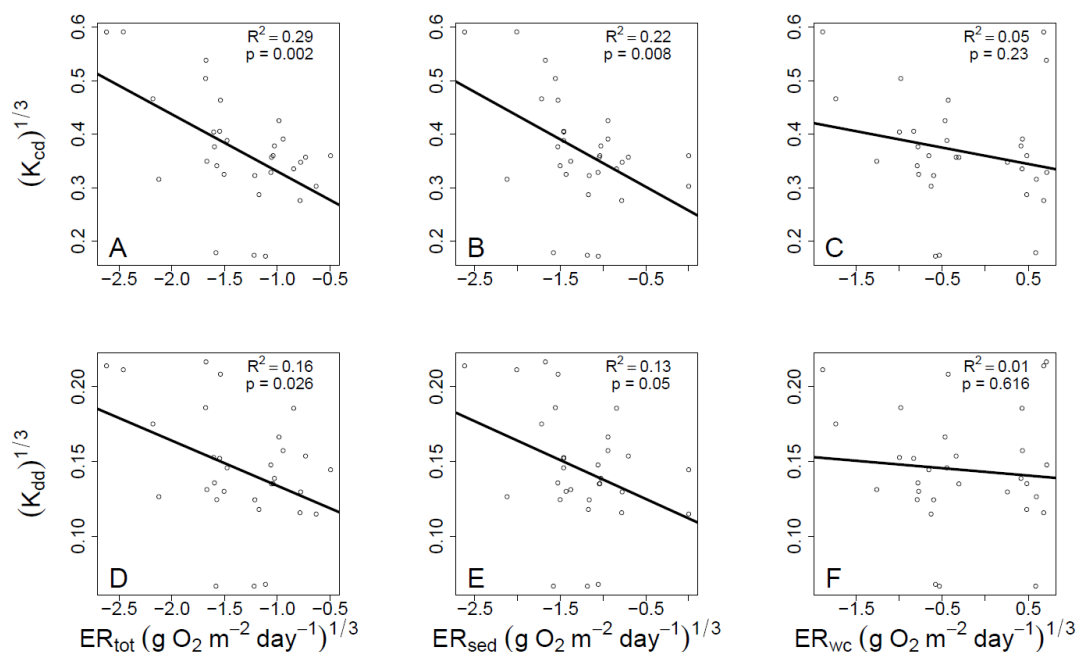
559

560 **Figure 4. Decay rates increase with drainage area.** K_{cd} (A) and K_{dd} (B) regressed against upstream
 561 drainage area and fit with an ordinary least squares linear regression. Associated regression models are
 562 shown as solid black lines and statistics are provided on each panel. Data were cube root transformed to
 563 improve normality before analysis.

564



565



566

567 **Figure 5: Decay rates related to each of the three aspects of stream ecosystem respiration.** Both K_{cd} (A-
 568 C) and K_{dd} (D-F) show strongest relationships with ER_{tot} (A,D), weaker relationships with ER_{sed} (B,E), and
 569 non-significant relationships with ER_{wc} (C,F). Ordinary least squares linear regression models are shown
 570 and solid black lines and associated statistics are provided on each panel. All variables were cube-root
 571 transformed to improve normality prior to regression analysis.

572



573 Tables

574 **Table 1.** Comparison of univariate and multivariate regression models explaining variation in K_{cd} and K_{dd} .
 575 Model structures are indicated, along with change in AIC relative to the best model. ER_{tot} was not used
 576 in multivariate models because $ER_{tot} = ER_{sed} + ER_{wc}$. Regression statistics for the univariate models are
 577 provided in Figure 5; only the best performing univariate models, in terms of R^2 , are shown. The models
 578 with ER_{sed} and ER_{wc} , but not the interaction term, are effectively the same as the ER_{tot} model because
 579 $ER_{tot} = ER_{sed} + ER_{wc}$. They are included as a point of reference for the model that also includes the
 580 $ER_{sed} * ER_{wc}$ interaction term.

Model	Δ AIC
$K_{cd} \sim ER_{tot}$	0
$K_{cd} \sim ER_{sed} + ER_{wc}$	3.8
$K_{cd} \sim ER_{sed} + ER_{wc} + ER_{sed} * ER_{wc}$	5.7
$K_{dd} \sim ER_{tot}$	0
$K_{dd} \sim ER_{sed} + ER_{wc}$	3.0
$K_{dd} \sim ER_{sed} + ER_{wc} + ER_{sed} * ER_{wc}$	4.8

581

582 **Table 2.** Regression coefficients from LASSO models explaining variation in K_{dd} and K_{cd} . Explanatory
 583 variables were cube root transformed to reduce influence from high leverage data points and
 584 standardized as z-scores to enable direct comparison of the regression coefficients. LASSO models were
 585 fit over 100 seeds. Regression coefficients (β) and R^2 values were averaged across the 100 seeds.
 586 Normalized regression coefficients were calculated by dividing each β coefficient by the maximum β
 587 coefficient in each seed. Standard deviation (sd) is reported for each variables' coefficient over the 100
 588 seeds and used to calculate the coefficient of variation (cv). Variables shown have an absolute value of
 589 mean normalized β of > 0.5 and $cv < 0.5$ to emphasize variables that were consistently important across
 590 seeds. Results for all variables, both normalized and not normalized, can be found in Table S1.

Response Variable	Predictor Variable	Mean Normalized Regression Coefficient (β)	sd	cv
K_{dd}	Water TDN	1	0	0
	D50	-0.699	0.087	-0.124
Mean R^2			0.502 (sd = 0.0673)	
K_{cd}	Aridity	-0.959	0.065	-0.067
	Water TDN	0.805	0.156	0.193
Mean R^2			0.883 (sd = 0.083)	

591

592

593

594

595